

# The Protective Role of Selenium on Scopolamine-Induced Memory Impairment, Oxidative Stress, and Apoptosis in Aged Rats: The Involvement of TRPM2 and TRPV1 Channels

Hasan Balaban<sup>1</sup> · Mustafa Nazıroğlu<sup>2,3</sup> · Kadir Demirci<sup>1</sup> · İshak Suat Övey<sup>2</sup>

Received: 12 February 2016 / Accepted: 4 March 2016 / Published online: 28 March 2016  
© Springer Science+Business Media New York 2016

**Abstract** Inhibition of Ca<sup>2+</sup> entry into the hippocampus and dorsal root ganglion (DRG) through inhibition of *N*-methyl-D-aspartate (NMDA) receptor antagonist drugs is the current standard of care in neuronal diseases such as Alzheimer's disease, dementia, and peripheral pain. Oxidative stress activates Ca<sup>2+</sup>-permeable TRPM2 and TRPV1, and recent studies indicate that selenium (Se) is a potent TRPM2 and TRPV1 channel antagonist in the hippocampus and DRG. In this study, we investigated the neuroprotective properties of Se in primary hippocampal and DRG neuron cultures of aged rats when given alone or in combination with scopolamine (SCOP). Thirty-two aged (18–24 months old) rats were divided into four groups. The first and second groups received a placebo and SCOP (1 mg/kg/day), respectively. The third and fourth groups received intraperitoneal Se (1.5 mg/kg/ over day) and SCOP + Se, respectively. The hippocampal and DRG neurons also were stimulated in vitro with a TRPV1 channel agonist (capsaicin) and a TRPM2 channel agonist (cumene hydroperoxide). We found that Se was fully effective in reversing SCOP-induced TRPM2 and TRPV1 current densities as well as errors in working memory and reference memory. In addition, Se completely reduced SCOP-induced oxidative toxicity by modulating lipid peroxidation, reducing glu-

tathione and glutathione peroxidase. The Se and SCOP + Se treatments also decreased poly (ADP-ribose) polymerase activity, intracellular free Ca<sup>2+</sup> concentrations, apoptosis, and caspase 3, caspase 9, and mitochondrial membrane depolarization values in the hippocampus. In conclusion, the current study reports on the cellular level for SCOP and Se on the different endocytotoxic cascades for the first time. Notably, the research indicates that Se can result in remarkable neuroprotective and memory impairment effects in the hippocampal neurons of rats.

**Keywords** Apoptosis · TRPV1 · TRPM2 · Selenium · Oxidative stress · Dementia

## Abbreviations

[Ca <sup>2+</sup> ] <sub>i</sub>	Intracellular free calcium ion
ACA	<i>N</i> -( <i>p</i> -Amylcinnamoyl)anthranilic acid
CAP	Capsaicin
CHPx	Cumene hydroperoxide
CPZ	Capsazepine
DMSO	Dimethyl sulfoxide
DRG	Dorsal root ganglion
EGTA	Ethylene glycol-bis[2-aminoethyl-ether]- <i>N,N,N,N</i> -tetraacetic acid
GSH	Reduced glutathione
GSH-Px	Glutathione peroxidase
HBSS	Hank's buffered salt solution
PARP	Poly (ADP-ribose) polymerase
RAM	radial arm-maze
RME	Reference memory error
ROS	Reactive oxygen species
SCOP	Scopolamine
TRP	Transient receptor potential
TRPM2	Transient receptor potential Mu

✉ Mustafa Nazıroğlu  
mustafanaziroglu@sdu.edu.tr

<sup>1</sup> Department of Psychiatry, Faculty of Medicine, Suleyman Demirel University, Isparta, Turkey

<sup>2</sup> Department of Neuroscience, Institute of Health Science, Suleyman Demirel University, Isparta, Turkey

<sup>3</sup> Neuroscience Research Center, University of Suleyman Demirel, TR-32260, Isparta, Turkey

TRPV1	Transient receptor potential vanilloid 1
WC	Whole cell
WME	Working memory error

## Introduction

Alzheimer's disease (AD) is a progressive neurodegenerative disorder causing dementia [1]. Researches have shown that the progressive nature of AD neurodegeneration leads to senile plaques, neurofibrillary tangles, intracellular  $\text{Ca}^{2+}$  dysregulation, disruption of synapses, and loss of neurons in brain cortical areas [1, 2]. In addition to the brain region, AD and other dementia also affect patients' dorsal root ganglion (DRG) neurons. Studies have observed perturbations of  $\text{Ca}^{2+}$  homeostasis caused by excessive levels of oxidative stress in AD patients' cells and in cells from animal models of the disease [3, 4]. It is well known that  $\text{Ca}^{2+}$  is an important messenger, playing a crucial role in regulating many physiological activities, such as cell viability, apoptosis, and synaptic plasticity [5, 6]. The role of cellular and molecular pathophysiology of overloaded  $\text{Ca}^{2+}$  influx and memory injury-induced DRG and hippocampal oxidative injury remains unclear despite research suggesting associations with dementia and AD, including beta amyloid plaque-induced oxidative stress (Graphical abstract) [7–9].

Oxidative stress plays an important role in the ethiopathogenesis of diseases with memory injury, such as AD and dementia [7–9]. One of the most accepted hypotheses for memory injury onset implicates mitochondrial dysfunction and oxidative stress as primary events in the pathology insurgence [2]. There is accumulating evidence suggesting that an overloaded intracellular free  $\text{Ca}^{2+}$  ( $[\text{Ca}^{2+}]_i$ ) concentration increases mitochondrial membrane depolarization, oxidative stress, and apoptotic pathways even though antioxidants control these pathways [10, 11]. Incorporated into the selenoproteins involved in antioxidant defenses, selenium is an essential dietary trace element acting as a cofactor for the glutathione peroxidase (GSH-Px) enzyme [12, 13]. Decreased blood selenium levels and GSH-Px activity were reported in patients with memory impairment [13, 14]. Selenium has been implicated as a neuroprotective agent in animal models of AD [15, 16]. The neuroprotective effects of selenium in DRG and hippocampal neurons are attributed to its ability to inhibit apoptosis [17] and to modulate  $\text{Ca}^{2+}$  influx through ion channels [18].

The  $\text{Ca}^{2+}$ -permeable transient receptors (TRP) melastatin 2 (TRPM2) and vanilloid 1 (TRPV1) are part of the TRP family, members of the melastatin and vanilloid subfamilies, respectively. TRPV1 is activated by different stimuli, such as low pH and noxious heat ( $\geq 43$ ). TRPV1 is also activated by the pungent (capsaicin) nature of hot chili peppers [19]. On the other hand, poly (ADP-ribose) polymerase (PARP) pathways through the production of ADP-ribose and  $\text{NAD}^+$  serve an

important role in activating the TRPM2 channel [20]. Nonetheless, both TRPV1 and TRPM2 are activated and potentiated by reactive oxygen species (ROS) [21, 22]. TRPM2 and TRPV1 channels are primarily expressed in the DRG, dentate gyrus, and hippocampal CA1 and CA3 regions [23, 24]. Growing interest in the therapeutic potential of TRPM2 and TRPV1 continually provides support for the hypothesis that TRPM2 and TRPV1 channel inhibition likely underlies many of the benefits associated with decreased dementia and AD [25–27], including improved antioxidant, learning, and executive functions [28]. Activating TRPM2 and TRPV1 has repeatedly resulted in increased cytosolic free  $\text{Ca}^{2+}$ , oxidative stress, and apoptotic cell injury [18]. Recently, a modulator role of selenium on TRPV1 and TRPM2 channels was reported in the DRG and hippocampus of rats [18], human neutrophils, and cell lines [29, 30]. Therefore, selenium may modulate  $\text{Ca}^{2+}$  entry via TRPM2 and TRPV1 channels, thus affecting oxidative stress and apoptosis in the DRG and hippocampus of rats with memory impairment. This effect should be clarified in the DRG and hippocampus of rats with memory impairment.

The role of  $\text{Ca}^{2+}$  influx through NMDA receptors on AD and dementia has been known for a long time [1, 2]. However, there exists no report on  $\text{Ca}^{2+}$  influx through TRPM2 and TRPV1 channels in rats with memory impairment. The molecular mechanism(s) underlying neuronal injury through memory injury remains poorly understood. To address this gap, we tested the effects of selenium treatment on apoptosis, oxidative stress, and  $\text{Ca}^{2+}$  influx through TRPM2 and TRPV1 channels in the DRG and hippocampus of scopolamine (SCOP)-induced aged rats.

## Materials and Methods

### Chemicals

Fura-2-acetoxymethyl ester (Fura-2AM) was obtained from Calbiochem (Darmstadt, Germany). Roswell Park Memorial Institute (RPMI) 1640 medium, sodium selenite, scopolamine hydrobromide, reduced glutathione (GSH), *N*-acetyl-Asp-Glu-Val-Asp-7-amino-4-methylcoumarin (ACDEVD-AMC), nonidet-P-40 substitute (NP40), 2-(*N*-morpholino)ethanesulfonic acid hydrate (MES hydrate), polyethylene glycol (PEG), penicillin-streptomycin, 4-(2-hydroxyethyl)-1-piperazineethanesulfonic acid (HEPES), 3-[(3 cholamidopropyl)dimethylammonio]-1-propanesulfonate (CHAPS), cumene hydroperoxide (CHPx), dimethyl sulfoxide (DMSO), PARP,  $\beta$ -actin, and dithiothreitol (DTT) were purchased from Sigma (Sigma Chemical Co., St. Louis, MO, USA). Dihydrorhodamine-123 (DHR-123), dimethyl sulfoxide, and Tris-glycine gels were from Molecular Probes (Eugene, OR, USA). His-Asp-7-amino-4-

methylcoumarin (AC-LEHD-AMC) was obtained from Bachem (Bubendorf, Switzerland). Dulbecco modified Eagle medium (DMEM) was purchased from Gibco (Istanbul, Turkey).

### Animals and Groups

The study used 32 (18–24 months) old female Wistar albino rats weighing  $320 \pm 30$  g at the start of the experiment. The animals were housed in a room with a temperature of  $22 \pm 2$  °C and humidity at 60 %. The environment included light control with a 12-h cycle starting at 08:00 h. The rats were fed with commercial food and allowed to drink water ad libitum. The 32 rats received radial arm-maze (RAM) task education for 14 days before starting, and their working memory (WME) and reference memory errors (RME) were recorded. During the experiments, three rats were not able to learn the radial arm-maze task during the education procedure, so they were exchanged for new rats prior to starting the study. The aged rats were divided into four groups (eight animals per group): (1) the control group, which received 1 ml of physiological saline treatment (0.9 % NaCl) per day; (2) the SCOP-alone-treated group for 21 days; (3) the selenium (Se)-alone-treated group for 14 days; and (4) the SCOP-treated group receiving Se treatment (SCOP+Se). Scopolamine hydrobromide was dissolved in an isotonic saline solution (0.9 % NaCl), and 1 mg/kg SCOP was intraperitoneally (IP) injected into the rats for 21 days [31]. Se (as sodium selenite at 1.5 mg/kg every other day) also was IP administered alone for 14 days [18]. The SCOP+Se group first received SCOP for 3 weeks, and then they IP received Se for 14 days (Fig. 1).

SCOP-induced memory impairment was used in the current study because it is one of the most widely used models without necessitating complex surgical procedures [32]. All research procedures and animal care complied with the guidelines of the International Association Study Plan for induction of memory injury. The study was approved by the Local Experimental Animal Ethical Committee of Suleyman Demirel University (SDU) (protocol number 10.02.2015-03). The animals were maintained and used according to the Animal Welfare Act and the Guide for the Care and Use of Laboratory.

At the end of each experiment, all rats were killed under ether anesthesia by cardiac blood taking in accordance with SDU experimental animal legislation. The DRG and hippocampal samples were isolated as described in a previous study [18]. At the end of the experiments, the DRG and half of the hippocampal samples were immediately used for patch-clamp and  $\text{Ca}^{2+}$  signaling analyses. The remaining hippocampal neurons were washed with phosphate buffer (pH 7.2) and frozen at  $-33$  °C. Western blot, GSH, GSH-Px, and lipid peroxidation analyses were performed within 1 month.

### Radial Arm-Maze Task

As previously reported, spatial memory testing was carried out using a radial arm-maze task [33]. The rats were individually tested for spatial memory during a 21-day training, and WME and RME were recorded. The animals were kept in the test device for a maximum of 10 min.

### Electrophysiology

Patch-clamp techniques have been described in detail elsewhere [18, 29]. With the patch-clamp technique in the whole-cell mode, DRG neurons were studied using an EPC10 patch-clamp set (HEKA, Lamprecht, Germany). Access cell resistances of whole-cell recording electrodes were 3–7 M $\Omega$ . The standard extracellular bath solution and pipette solutions were used in previous studies [18, 29]. For  $\text{Na}^+$  free solution of extracellular buffer,  $\text{Na}^+$  was replaced by 150-mM *N*-methyl-D-glucamine (NMDG<sup>+</sup>) and the pH was adjusted with HCl. The osmolarity of the solution was 310 mOsmol/L. It is well known that TRPM2 channels are activated in the presence of high  $[\text{Ca}^{2+}]_i$  concentration.  $[\text{Ca}^{2+}]_i$  in TRPM2 experiments was set to 1  $\mu\text{M}$  (0.886 mM  $\text{Ca}^{2+}$ , 1 mM Cs-EGTA) instead of 100 nM  $\text{Ca}^{2+}$ . The  $\text{Ca}^{2+}$  concentrations of the intracellular and extracellular solutions were calculated by using the MAXC program (<http://www.stanford.edu/cpatton/maxc.html>).

The DRG neurons were held at a potential of  $-60$  mV, and current–voltage (*I*–*V*) relationships were obtained from voltage ramps from  $-90$  to  $+60$  mV applied over 400 ms. In the patch-clamp experiments, TRPM2 and TRPV1 channels were gated by adding extracellular  $\text{H}_2\text{O}_2$  (10 mM) and capsaicin (0.010 mM), and they were blocked by extracellular (in bath of patch chamber) *N*-(*p*-amylcinnamoyl)anthranilic acid (ACA, 0.04 mM) and capsazepine (CPZ). All experiments were done at room temperature ( $21 \pm 2$  °C). For the analysis, the maximal current amplitudes (pA) in a DRG neuron were divided by the cell capacitance (pF), a measure of the cell surface. The results in the patch clamp experiments are the current density (pA/pF).

### Measurement of Intracellular Free Calcium Concentration

Intracellular free calcium  $[\text{Ca}^{2+}]_i$  was measured with the fluorescent indicator Fura-2-AM [34]. To measure, cells were trypsin-digested, allowed to sediment, re-suspended in HEPES-buffered medium, consisting of 20 mM HEPES (pH 7.4), 10 mM NaCl, 4.8 mM KCl, 1.2 mM  $\text{KH}_2\text{PO}_4$ , 1.2 mM  $\text{MgSO}_4$ , 0.5 mM  $\text{CaCl}_2$ , 25 mM  $\text{NaHCO}_3$ , 15 mM glucose, and 0.1 % bovine serum albumin (fatty acid free), and then loaded with 5  $\mu\text{M}$  fura-2AM for 45 min. Fluorescence was recorded from 2-ml aliquots of magnetically stirred cellular

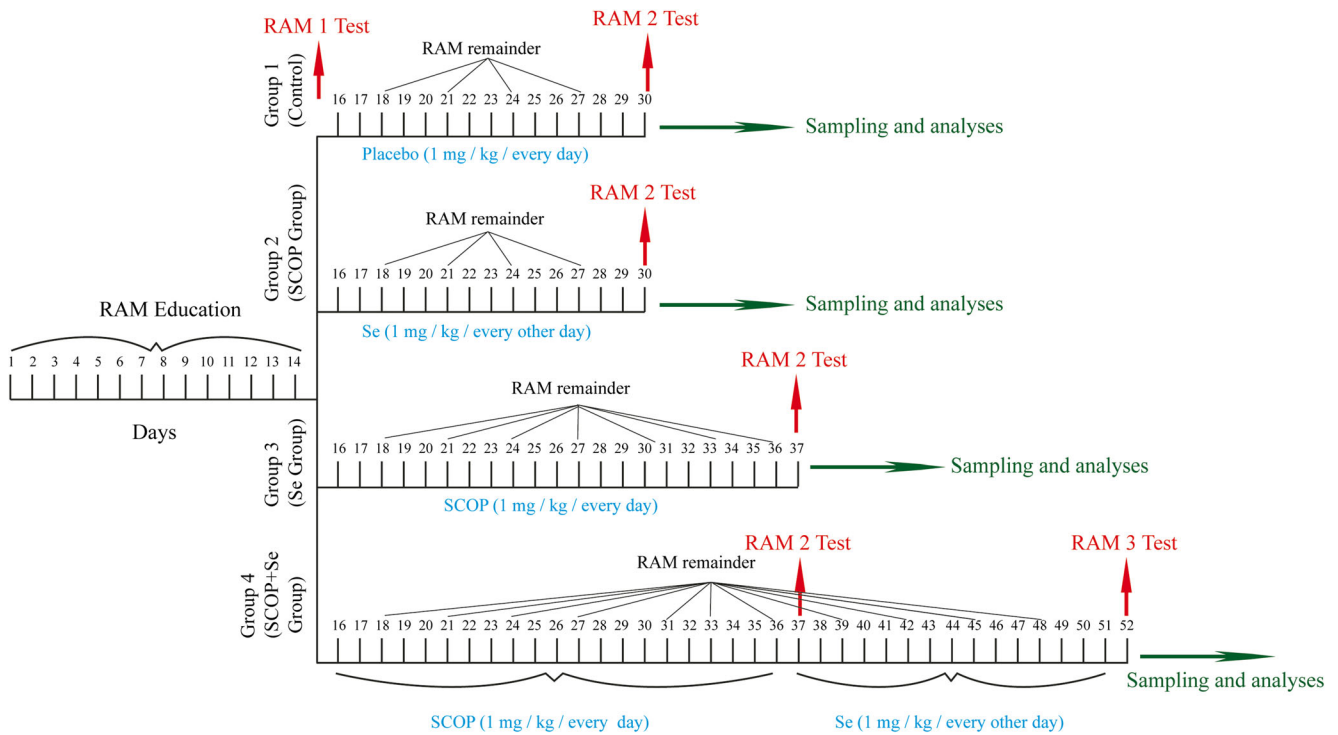


**Fig. 1** Experimental and treatment designs of rats

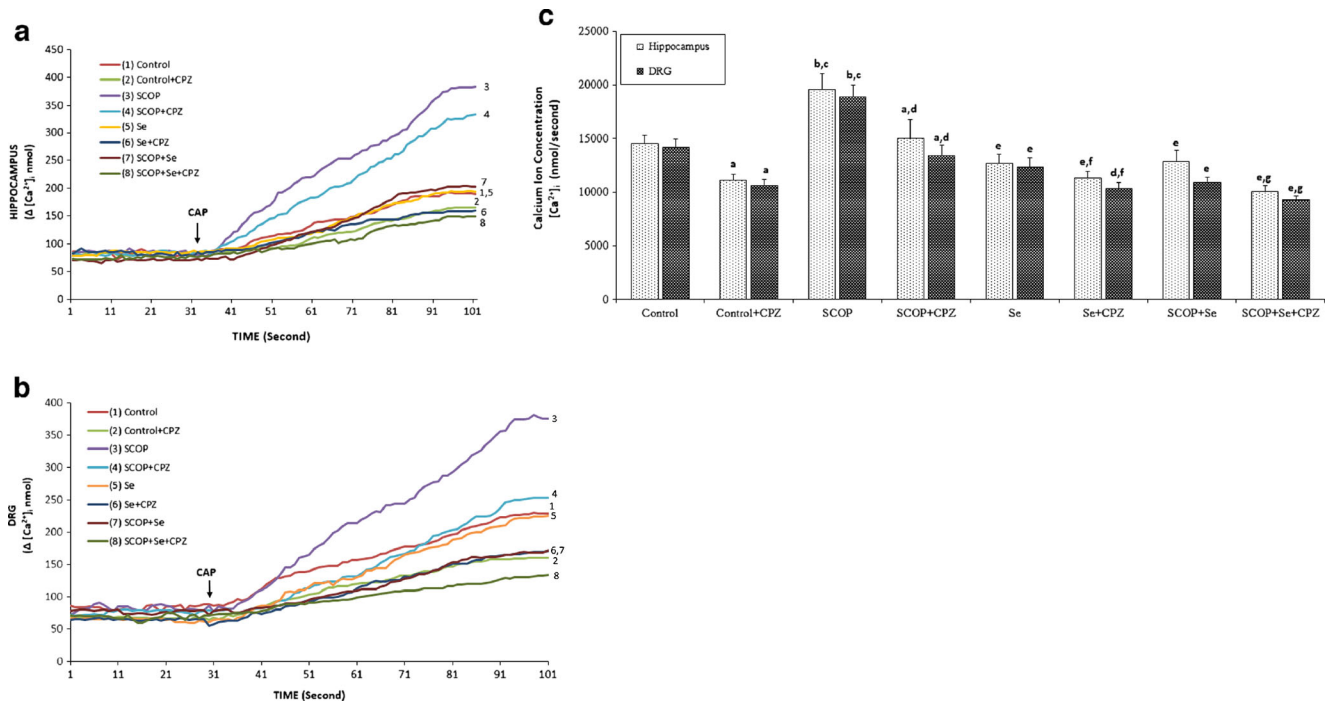


**Fig. 2** Effects of selenium (Se) treatment on  $[Ca^{2+}]_i$  through TRPV1 channel in hippocampal (a) and DRG (b) neurons in control and rats with scopolamine (SCOP)-induced memory injury ( $n=8$  and mean  $\pm$  SD). The animals received intraperitoneal SCOP and Se. These neurons were dissected from control and treated animals. Fura-2-loaded rat hippocampal and DRG neurons in the four groups were further treated

with capsaicin (CAP and 0.01 mM) in the presence of normal extracellular calcium (1.2 mM) for 100 s. The TRPV1 channels in the neurons were inhibited by capsazepine (CPZ and 0.1 mM). (<sup>a</sup> $p < 0.05$  and <sup>b</sup> $p < 0.001$  versus control. <sup>c</sup> $p < 0.05$  versus control + CPZ group. <sup>d</sup> $p < 0.05$  and <sup>e</sup> $p < 0.001$  versus SCOP group. <sup>f</sup> $p < 0.05$  versus Se group. <sup>g</sup> $p < 0.05$  versus SCOP + Se group) (Fig. 1c)



suspensions at 37 °C by using a spectrofluorometer (Carry Eclipse, Varian Inc, Sydney, Australia) with excitation wavelengths of 340 and 380 nm and emission at 505 nm. Changes in  $[Ca^{2+}]_i$  were monitored by using the Fura-2 340/380 nm fluorescence ratio and were calibrated according to the method of Grynkiewicz [35].

$Ca^{2+}$  release in the DRG and hippocampal neurons were estimated using the integral of the rise in  $[Ca^{2+}]_i$  for the first 100 s after adding capsaicin (0.1 mM) or CHPx (0.1 mM).  $Ca^{2+}$  release is expressed in nanomolar quantities by taking a sample every second as previously described [36, 37]. In some experiments, the neurons were incubated with ACA (0.04 mM and 1 min) and CPZ (0.1 mM and 30 min) before measuring the concentration of  $[Ca^{2+}]_i$ .

### Intracellular ROS Production Measurement

Rhodamine 123 (Rh 123) is a nonfluorescent, noncharged dye that easily penetrates cell membranes. Once inside the cell, DHR 123 becomes fluorescent upon oxidation to Rh 123, with the fluorescence being proportional to ROS generation. Succinctly, the hippocampal neurons ( $10^6$  cells/ml) were washed with serum-free RPMI 1640 medium and incubated with 0.02-mM DHR 123 at 37 °C for 25 min [37, 38]. The

fluorescence intensity of Rh 123 was measured (excitation 488 nm and emission 543 nm) in an automatic microplate reader (Infinite 200 PRO; Tecan Austria GmbH, Groedig, Austria). Data are presented as fold increase over the pretreatment level (experimental/control).

### Determination of Mitochondrial Membrane Potential

JC-1 was used to determine the mitochondrial membrane potential ( $\Delta\Psi_m$ ) [37]. The hippocampal neurons were incubated with JC-1 at 37 °C for 45 min. JC-1 fluorescence was measured by a single excitation wavelength (488 nm) with dual emission, green (520 nm) and red (596 nm) using the microplate reader (Infinite 200 PRO). The value of  $\Delta\Psi_m$  is calculated as the ratio of red to green fluorescence. The relative transmembrane potential was expressed as a percentage of  $\Delta\Psi_m$  relative to vehicle control (fold increase).

### Assay for Apoptosis Level and Caspase 3 and Caspase 9 Activities

The apoptosis assay was performed using a commercial kit according to the instructions provided by Biocolor Ltd (Northern Ireland) and elsewhere [18]. When the membrane

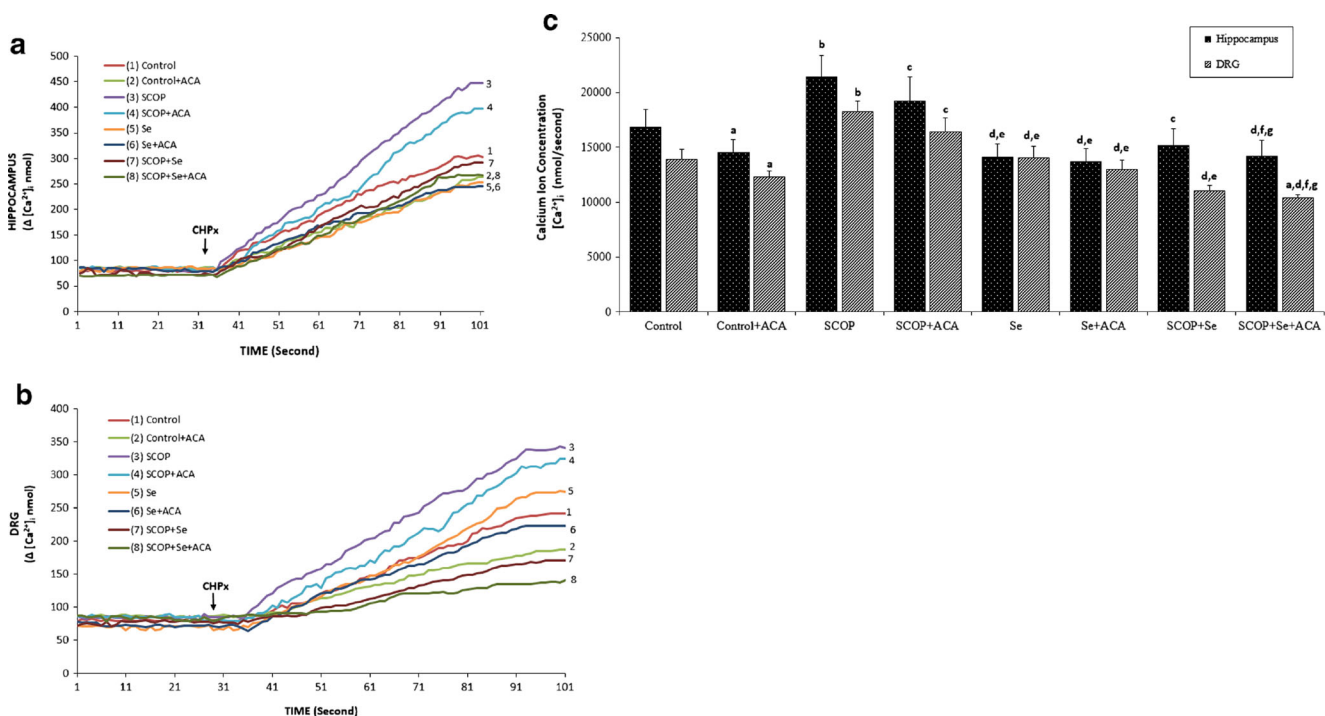


**Fig. 3** Effects of selenium (Se) treatment on  $[Ca^{2+}]_i$  through TRPM2 channel in hippocampal (a) and DRG (b) neurons in control and rats with scopolamine (SCOP)-induced memory injury ( $n = 8$  and mean  $\pm$  SD). The animals received intraperitoneal SCOP and Se. These neurons were dissected from control and treated animals. Fura-2-loaded rat hippocampal neurons were further treated with TRPM2 agonist

cumene hydroperoxide (CHPx and 1 mM) in the presence of normal extracellular calcium (1.2 mM) for 100 s. The TRPM2 channels in the neurons were inhibited by ACA (0.04 mM). (<sup>a</sup> $p < 0.05$  and <sup>b</sup> $p < 0.001$  versus control. <sup>c</sup> $p < 0.05$  and <sup>d</sup> $p < 0.001$  versus SCOP group. <sup>e</sup> $p < 0.05$  and <sup>f</sup> $p < 0.001$  versus SCOP + ACA. <sup>g</sup> $p < 0.05$  versus Se group) (Fig. 2c)

of the apoptotic cell loses its asymmetry, the APOPercentage dye is actively transported into cells, staining apoptotic cells red, thus allowing detection of apoptosis by spectrophotometer [12].

The determinations of caspase 3 and caspase 9 activities in hippocampus were based on methods previously reported [37, 38] with minor modifications. Stimulated or resting cells were washed once with PBS. Fifteen microliters of the neuron suspension ( $10^6$  cells/ml) were added to the microplate and mixed with the appropriate peptide substrate dissolved in a standard reaction buffer that was composed of 100 mM HEPES, pH 7.25, 10 % sucrose, 0.1 % CHAPS, 5 mM DTT, 0.001 % NP40, and 0.04 ml of caspase 3 substrate (AC-DEVD-AMC) or 0.1 M MES hydrate, pH 6.5, 10 % PEG, 0.1 % CHAPS, 5 mM DTT, 0.001 % NP40, and 0.1 mM of caspase 9 substrate (AC-LEHD-AMC). Substrate cleavage was measured with the microplate reader with excitation wavelength of 360 nm and emission at 460 nm. The data were calculated as fluorescence units per milligram protein and presented as fold increase over the pretreatment level (experimental/control).

#### Lipid Peroxidation, Reduced Glutathione, Glutathione Peroxidase, and Protein Assay

Spectrophotometric method of Placer et al. [39] was used for analyses of lipid peroxidation levels of the hippocampal neurons. Homogenates of hippocampal neurons were prepared in 50-mM phosphate buffer (pH 7.4) by an ultrasonic homogenator. The amount of malondialdehyde was measured by a spectrophotometer at 532 nm (UV-1800, Shimadzu, Kyoto, Japan). The values of lipid peroxidation in the neurons were expressed as micromoles per gram of protein.

The GSH concentration [40] and GSH-Px activity [41] of the hippocampal neurons were spectrophotometrically measured at 37 °C and 412 nm using the method described in our previous study [18]. The values of GSH and GSH-Px in the neurons were expressed as micromoles per gram of protein and International Unit per gram of protein, respectively. The total protein was assessed using Bradford's method, and bovine serum albumin was used as the standard for the analyses.

#### Western Blot Analyses

All Western blot analyses in the hippocampal neurons were performed using standard procedures [18]. Obtained bands were visualized using ECL Western HRP Substrate (Millipore Luminat Forte, USA), and visualization was achieved through Syngene G:BOX Gel Imagination System (UK) and normalized against  $\beta$ -actin protein. The data are presented as relative density (fold increase) over the pretreatment level (experimental/control).

**Fig. 4** Effects of selenium (Se) treatments on TRPV1 channel activation in the DRG of control and rats with scopolamine (SCOP)-induced memory injury. The holding potential was  $-60$  mV. **a** Control: original recordings from control neuron. **b** Control+CAP group: DRG was isolated from rats without SCOP administration, and they were stimulated by capsaicin (CAP and 0.01 mM) but inhibited by capsazepine (CPZ and 0.1 mM). **c** SCOP group: TRPV1 currents in the DRG neurons of SCOP-administrated rats were stimulated by CAP (0.01 mM) in the bath (chamber), and they were inhibited by CPZ (0.1 mM) in the bath. **d** Se group: The rats received intraperitoneal Se, and then the DRG neurons were stimulated by in vitro CAP. **e** SCOP+Se group: The rats received 2 weeks Se after induction of experimental dementia via SCOP, and then the DRG was stimulated by CAP. *B I–V* and *C I–V*: Current voltage relationships of whole-cell currents in the presence of various extracellular cations, activators, and inhibitors as indicated (same experiments as in panels **b**, **c**). *WC* whole cell

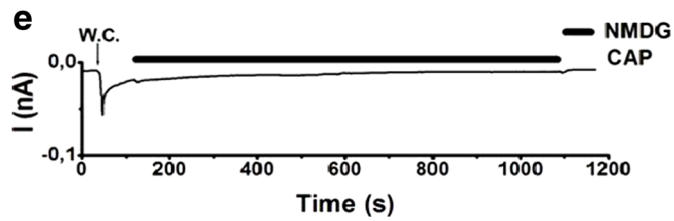
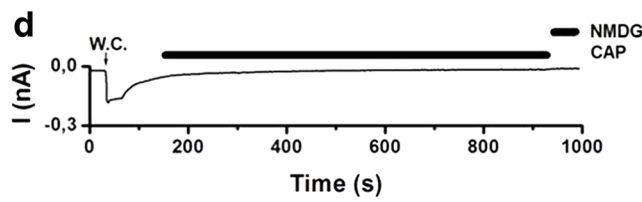
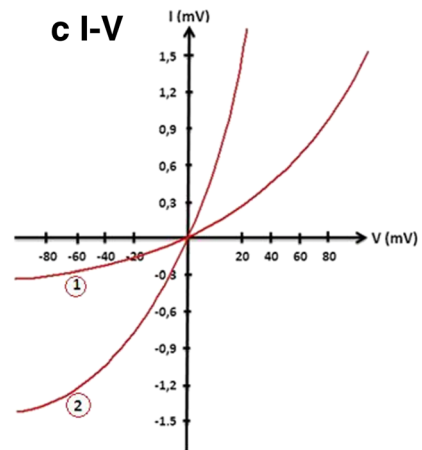
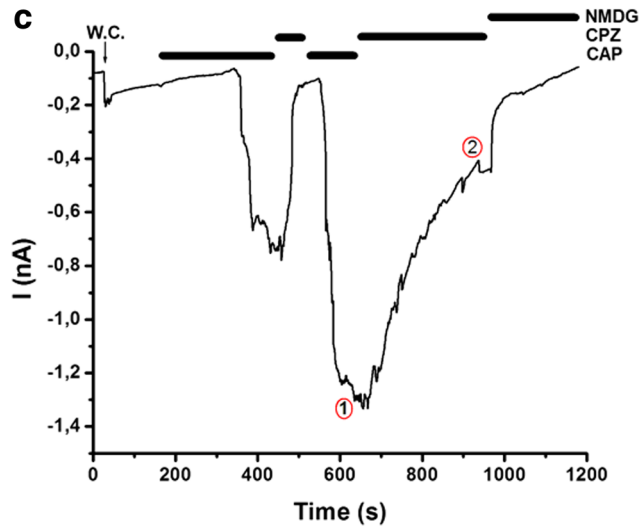
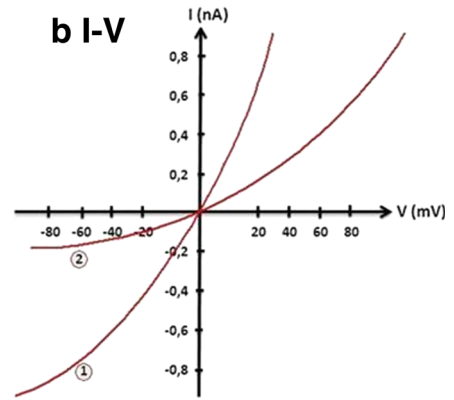
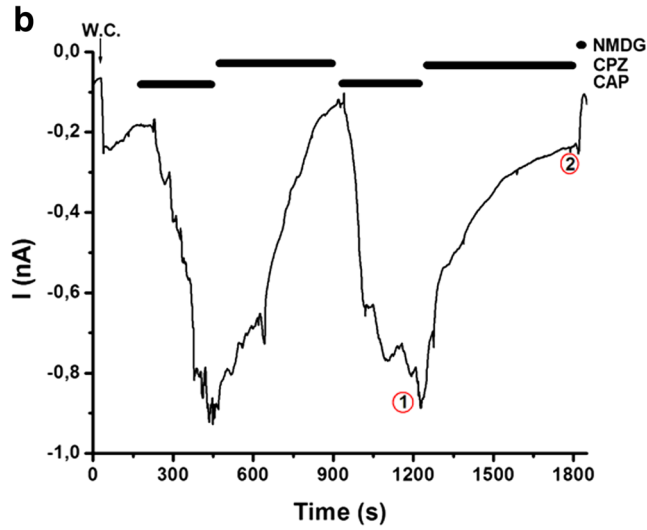
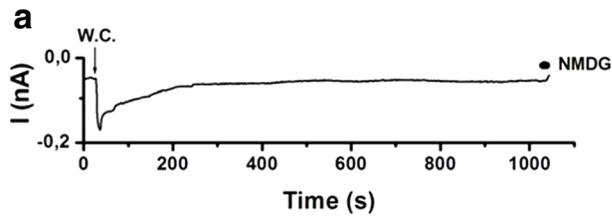
#### Statistical Analyses

All results were expressed as means  $\pm$  standard deviation (SD), and *p* values less than 0.05 were regarded as significant. To determine the effect of treatment, data were analyzed using ANOVA. Presence of significance was assessed with LSD test. The significant values in six groups were assessed with an unpaired Mann–Whitney *U* test. The SPSS statistical program was used to analyze the data (version 17.0 software, SPSS Inc., Chicago, IL, USA).

#### Results

##### The Effects of Selenium and SCOP Treatments on $[Ca^{2+}]_i$ Accumulation Through TRPV1 Channel Activity in the Hippocampus and DRG of Rats

CPZ is a specific TRPV1 receptor antagonist. This study used it in the SCOP-induced dementia model in order to identify the TRPV1 receptor involved in  $Ca^{2+}$  accumulation via TRPV1 channels. As shown in Fig. 2a–c, the  $[Ca^{2+}]_i$  in hippocampal and DRG neurons were significantly ( $p < 0.001$ ) lower in the control+CPZ group compared to the control animals. However,  $[Ca^{2+}]_i$  was also markedly ( $p < 0.001$ ) higher in the SCOP group when compared to the control group. We also observed a modulator role for CPZ on the  $[Ca^{2+}]_i$  in the neurons. Its concentration was significantly ( $p < 0.05$ ) lower in the SCOP+CPZ and Se+CPZ groups than in the SCOP and Se groups, respectively.  $Ca^{2+}$  entry through inhibition of TRPV1 channel activity was further decreased by the selenium treatments, and  $[Ca^{2+}]_i$  was also significantly ( $p < 0.05$ ) lower in the Se+CPZ and SCOP+Se+CPZ than in the only Se and SCOP+Se groups, respectively (Fig. 2c).



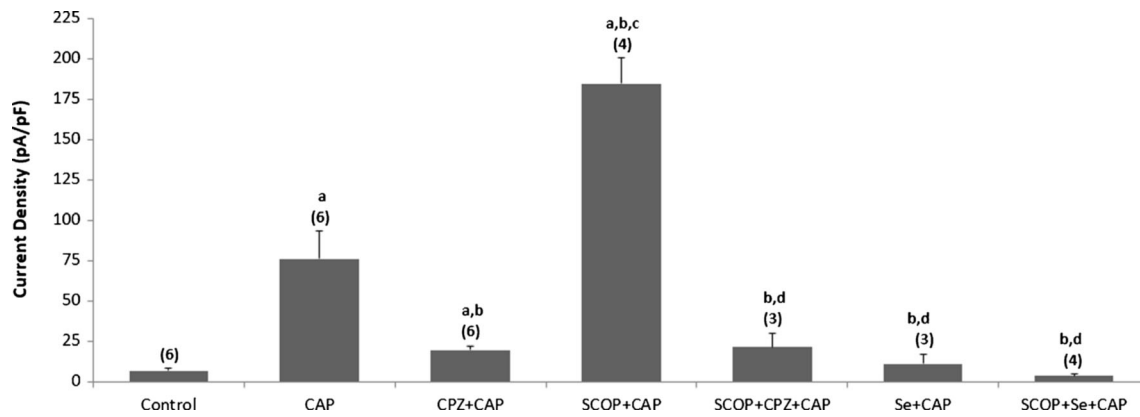


**Fig. 5** Role of selenium (Se) treatment on TRPV1 channel capacitance of the DRG in control and rats with scopolamine (SCOP)-induced memory injury. The DRG neurons were dissected from *in vivo* treated animals, and they were further treated *in vitro* afterwards with CAP (0.01 mM) and CPZ (0.1 mM). For each of the applications, the initial current density (divided by the cell capacitance, a measure of cell size)

was calculated after administration of CAP (mean  $\pm$  SD). The numbers in parentheses indicate *n* number of groups. Significant stimulation and inhibition of currents are indicated with letters. <sup>a</sup> $p < 0.001$  versus control. <sup>b</sup> $p < 0.001$  versus CAP group. <sup>c</sup> $p < 0.001$  versus CPZ + CAP group. <sup>d</sup> $p < 0.001$  versus SCOP group

### The Effects of Selenium and SCOP Treatments on $[Ca^{2+}]_i$ and TRPM2 Channel Activation in the DRG and Hippocampus of Rats

Within nonspecific agonists of the TRPM2 channel, ACA is the best TRPM2 receptor antagonist, and we used it in the SCOP-induced memory injury model to identify the TRPM2 involved in calcium accumulation. As shown in Fig. 3a (hippocampal neurons), b (DRG neurons), and c,  $[Ca^{2+}]_i$  in hippocampal and DRG neurons were significantly ( $p < 0.001$ ) higher in the SCOP group as compared to the control group.  $[Ca^{2+}]_i$  was significantly ( $p < 0.001$ ) lower in the Se and SCOP + Se groups than in the SCOP groups.  $[Ca^{2+}]_i$  concentration was also significantly ( $p < 0.001$ ) lower in the control + ACA, SCOP + ACA, and Se + ACA groups than in the SCOP groups. Compared to the Se and SCOP + Se groups,  $[Ca^{2+}]_i$  was also further ( $p < 0.05$ ) decreased in the SCOP + Se + ACA groups and Se + ACA groups by ACA treatments.

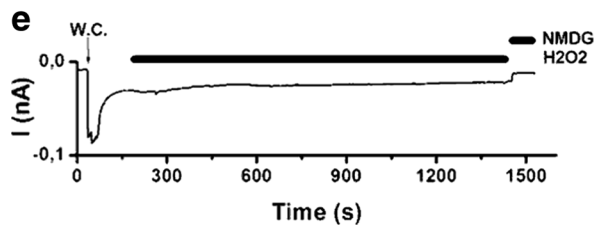
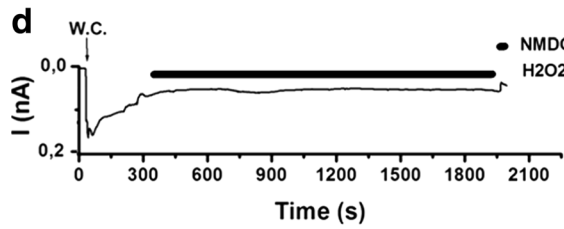
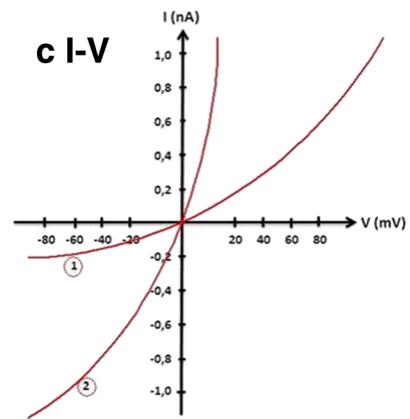
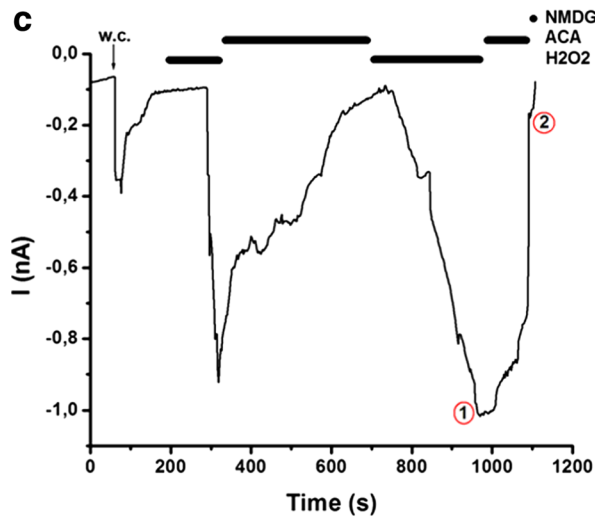
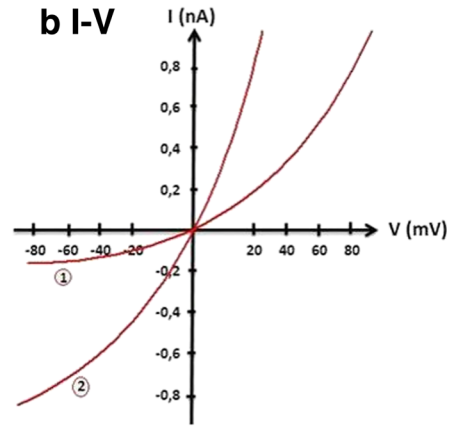
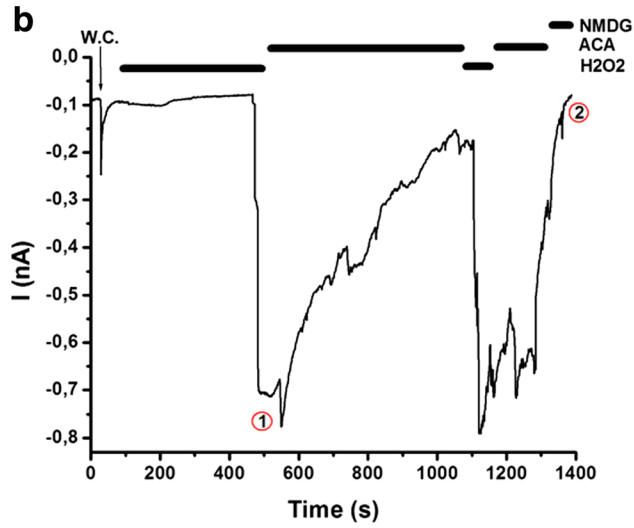
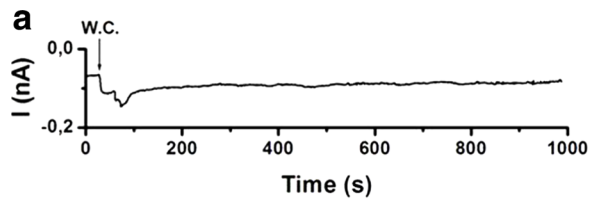
### The Effects of Selenium on TRPV1 Channel in the DRG of Rats with Scopolamine-Induced Memory Impairment

Figures 4 and 5 demonstrate the effects of SCOP and selenium on TRPV1 channels activated by capsaicin. Capsaicin (0.01 mM) induced a current in native DRG neurons (Fig. 4b). Reaching amplitudes of well above 0.90 nA, the currents induced by capsaicin developed gradually (between 1.15 and 1.35 min) following the addition of capsaicin to the medium. These currents were reversibly and partially blocked by CPZ and NMDG<sup>+</sup> (see Fig. 4b, c). We observed no current in the absence of capsaicin (Fig. 4a). We obtained control data every experimental day using the same animals as those used for studying TRPV1. In the absence of capsaicin, the mean value for the current densities in the control DRG neurons was

6.69 pA/pF ( $n = 6$ ) ( $-60$  mV holding potential). The mean values of the current densities in the CAP, CPZ + CAP, SCOP, and SCOP + CAP groups as pA/pF were 75 ( $n = 6$ ), 19 ( $n = 6$ ), 184 ( $n = 4$ ), and 21 ( $n = 3$ ), respectively. Current densities of the DRG neurons were significantly ( $p < 0.001$ ) decreased in the CAP and SCOP groups by CPZ treatments. In essence, we observed an activating role for SCOP on the TRPV1 current in DRG neurons. The current densities were also significantly ( $p < 0.001$ ) lower in the Se and SCOP + Se groups compared to the SCOP-only group, (Fig. 5), and selenium treatments decreased the values to control levels. Oxidative stress plays an important role in the etiology of memory impairment [5, 7]. It is well known that excessive production of ROS occurs in capsaicin-induced mitochondrial membrane depolarization and mitochondrial  $Ca^{2+}$  accumulation through activation of the TRPV1 channel. Nonetheless, CPZ induces antioxidant effects in the DRG and hippocampus of rats via modulation of TRPV1 channel activity and

**Fig. 6** Effects of selenium (Se) treatments on TRPM2 channel activation in the DRG of control and rats with scopolamine (SCOP)-induced memory injury. The holding potential was  $-60$  mV. **a** Control: original recordings from control neuron. **b** Control +  $H_2O_2$  group: DRG was isolated from rats without SCOP administration, and they were stimulated by capsaicin (CAP and 0.01 mM) but inhibited by capsazepine (CPZ and 0.1 mM). **c** SCOP group: TRPV1 currents in the DRG neurons of SCOP-administrated rats were gated by  $H_2O_2$  (10 mM) in the patch chamber, and they were inhibited by ACA (0.04 mM) in the bath of patch chamber. **d** Se group: The rats received intraperitoneal Se, and then the DRG neurons were stimulated by *in vitro*  $H_2O_2$  (10 mM). **e** SCOP + Se group: The rats received 2 weeks Se after induction of experimental memory injury via SCOP, and then the DRG was stimulated by  $H_2O_2$  (10 mM). **B** I–V and **C** I–V: current voltage relationships of whole-cell currents in the presence of various extracellular cations, activators, and inhibitors as indicated (same experiments as in panels b, c). WC whole cell





cytosolic  $\text{Ca}^{2+}$  [18]. As a result, we observed capsaicin-evoked TRPV1 currents in neurons due to an increase in effective agonist concentration, presumably due to chemical reactions between the antioxidant selenium and ROS.

### The Effects of Selenium on TRPM2 Channel in the DRG of Rats with Scopolamine-Induced Memory Impairment

Figures 6 and 7 show effects of Se and SCOP on TRPM2 channels activated by  $\text{H}_2\text{O}_2$ . TRPM2 currents induced by  $\text{H}_2\text{O}_2$  developed gradually (within  $1.71 \pm 0.18$  min) following infusion of  $\text{H}_2\text{O}_2$  to neurons' cytosol, reaching amplitudes (at a holding potential of  $-60$  mV) of well above  $0.78$  nA. These currents were reversibly blocked by the TRPM2 channel antagonist, ACA, and  $\text{NMDG}^+$  as a substitute ion for  $\text{Na}^+$  (see Fig. 6b, c). We obtained control data every experimental day using the same animals as those used for studying TRPM2, observing no current in the absence of  $\text{H}_2\text{O}_2$  (Fig. 6a). In the control DRG neurons, the mean values for the current densities in the absence of  $\text{H}_2\text{O}_2$  was  $3.41$  pA/pF ( $n=7$ ). The mean values of the current densities (as pA/pF) of the DRG neurons were significantly ( $p<0.001$ ) higher in the control+ $\text{H}_2\text{O}_2$  and SCOP+ $\text{H}_2\text{O}_2$  groups than in the control groups. Nonetheless, ACA treatments significantly ( $p<0.001$ ) decreased mean values in the control+ACA+ $\text{H}_2\text{O}_2$  and SCOP+ACA+ $\text{H}_2\text{O}_2$  groups (Fig. 7). In addition, selenium treatment decreased current densities for the Se+ $\text{H}_2\text{O}_2$  and SCOP+Se+ $\text{H}_2\text{O}_2$  groups to control levels; the densities were markedly lower in the Se+ $\text{H}_2\text{O}_2$  and SCOP+Se+ $\text{H}_2\text{O}_2$  groups than in the control+ $\text{H}_2\text{O}_2$  and SCOP+ $\text{H}_2\text{O}_2$  groups.

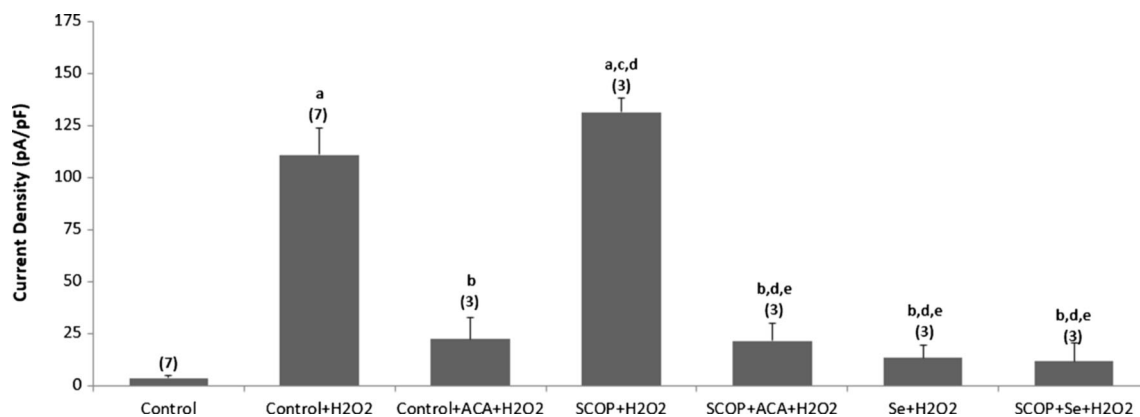


**Fig. 7** Role of selenium (Se) treatment on TRPM2 channel capacitance of the DRG in control and rats with scopolamine (SCOP)-induced memory injury. The DRG neurons were dissected from in vivo treated animals, and they were further treated in vitro afterwards with  $\text{H}_2\text{O}_2$  (10 mM) and ACA (0.04 mM). For each of the applications, the initial current density (divided by the cell capacitance, a measure of cell size)

### Results of Apoptosis, MTT, and Caspase 3 and Caspase 9 Values in Hippocampal Neurons of Rats with SCOP-Induced Memory Impairment

Figures 8 and 9 show the effects of selenium on SCOP-induced apoptosis, cell viability (MTT) levels, and caspase 3 and caspase 9 activities through TRPV1 (Figs. 8a and 9a) and TRPM2 (Figs. 8b and 9b) channel activation in the hippocampal neurons. The apoptosis levels and caspase 3 and caspase 9 activities were significantly ( $p<0.001$ ) higher in the SCOP groups than in the controls, although the MTT levels were markedly ( $p<0.001$ ) lower in the SCOP groups than in the controls. The SCOP-induced apoptosis levels and caspase 3 and caspase 9 activities significantly ( $p<0.05$ ) decreased in the SCOP+CPZ, Se, Se+CPZ, SCOP+Se, and SCOP+Se+CPZ groups through the CPZ and Se treatments, although MTT levels were markedly ( $p<0.05$ ) increased in the groups with the CPZ and Se treatments.

### Results of Mitochondrial Membrane Depolarization (JC-1) and Intracellular ROS Production in Hippocampal Neurons of Rats with SCOP-Induced Memory Impairment

We also investigated the protective effects of melatonin and selenium on JC-1 and ROS levels in the hippocampal (Fig. 10a) and DRG (Fig. 10b) neurons. The JC-1 and ROS levels in the hippocampal and DRG neurons were significantly ( $p<0.001$ ) higher in the SCOP groups than in the control. In addition, the JC-1 ( $p<0.05$ ) and ROS ( $p<0.001$ ) levels in the hippocampal and DRG neurons were also significantly

was calculated after administration of CAP (mean  $\pm$  SD). The numbers of group were indicated in parentheses. Significant stimulation and inhibition of currents are expressed by letters. <sup>a</sup> $p<0.001$  versus control. <sup>b</sup> $p<0.001$  and <sup>c</sup> $p<0.05$  versus control+ $\text{H}_2\text{O}_2$  group. <sup>d</sup> $p<0.001$  versus control+ACA+ $\text{H}_2\text{O}_2$  group. <sup>e</sup> $p<0.001$  versus SCOP+ $\text{H}_2\text{O}_2$  group)

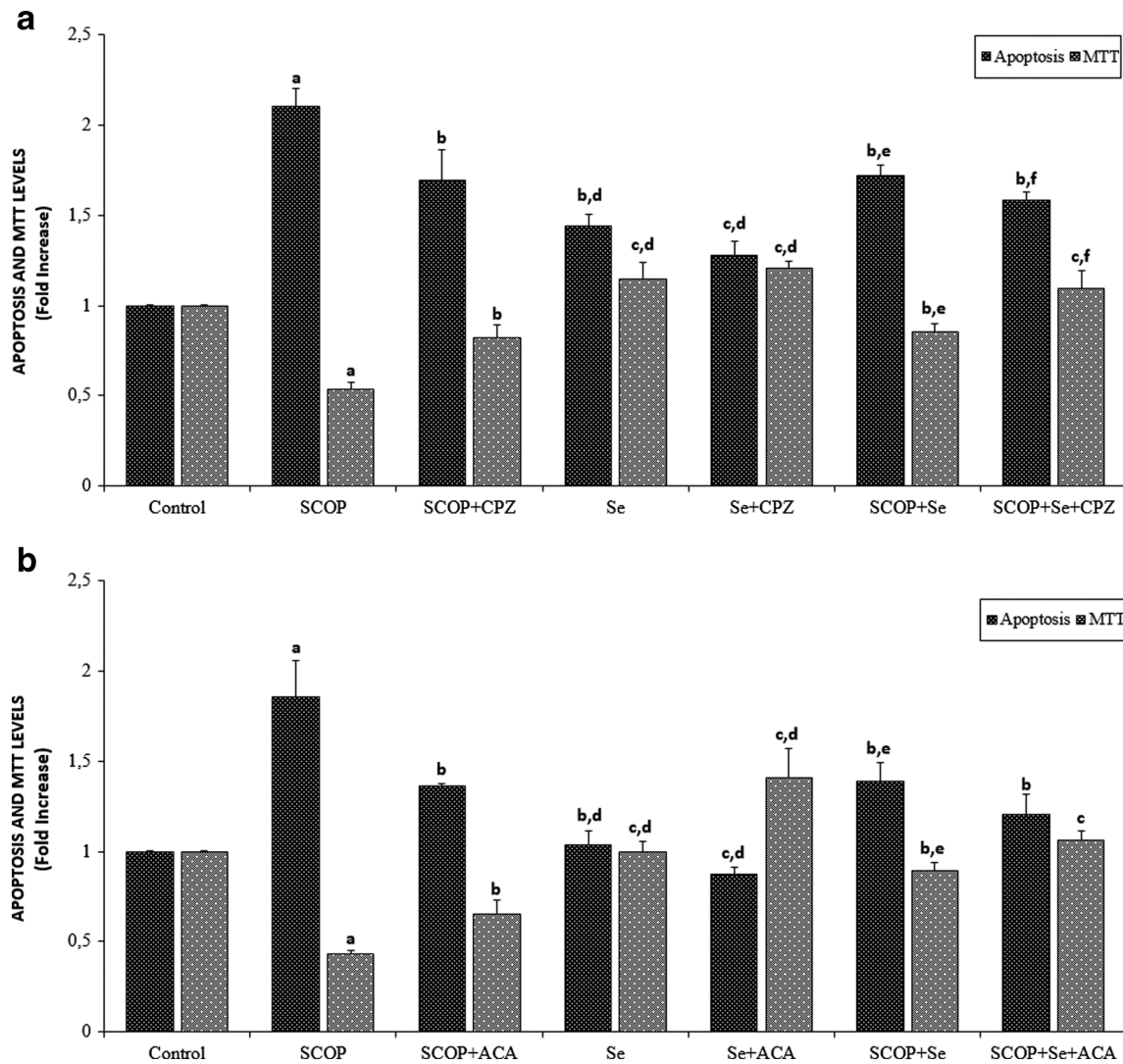


**Fig. 8** Effects of selenium (Se) and SCOP administrations on apoptosis and MTT levels through TRPV1 and TRPM2 channel activities in hippocampal neurons of rats ( $n=8$ ). The hippocampal neurons were dissected from in vivo treated animals, and they were further treated in vitro afterwards with capsaicin (0.01 mM) (a) and CHPx (1 mM) (b), although they were inhibited by CPZ (0.1 mM) and ACA

(0.04 mM), respectively. Values were expressed as fold increase over the pretreatment level (experimental/control). <sup>a</sup> $p < 0.001$  versus control. <sup>b</sup> $p < 0.05$  and <sup>c</sup> $p < 0.001$  versus SCOP group. <sup>d</sup> $p < 0.05$  versus SCOP + CPZ and SCOP + ACA groups. <sup>e</sup> $p < 0.05$  versus Se, Se + CPZ, and Se + ACA groups. <sup>f</sup> $p < 0.05$  versus SCOP + Se groups)

( $p < 0.05$ ) lower in the Se and SCOP + Se groups compared to the SCOP-only group.

### Results of Reference Memory Error and Working Memory Error Levels in RAM Tests of the Aged Rats

It is well known that RME in REM tests represents short memory impairment while WME represents long memory impairment in the brain [33]. Table 1 shows the RME and WME results. The memory error values increased in the SCOP group and significantly ( $p < 0.05$  for RME and  $p < 0.001$  for WME) increased in the

SCOP group between the first and second RAM tests. However, selenium treatments decreased the values in selenium and SCOP + selenium groups ( $p < 0.001$ ).

### The Effects of SCOP and Selenium on GSH-Px, GSH, and Lipid Peroxidation Values in the Hippocampal Neurons

Table 2 illustrates the effects of SCOP and selenium on GSH-Px, GSH, and lipid peroxidation values. Antioxidants including selenium are thought to play a pivotal role in protecting cells against ROS. Aging is an important source of oxidative

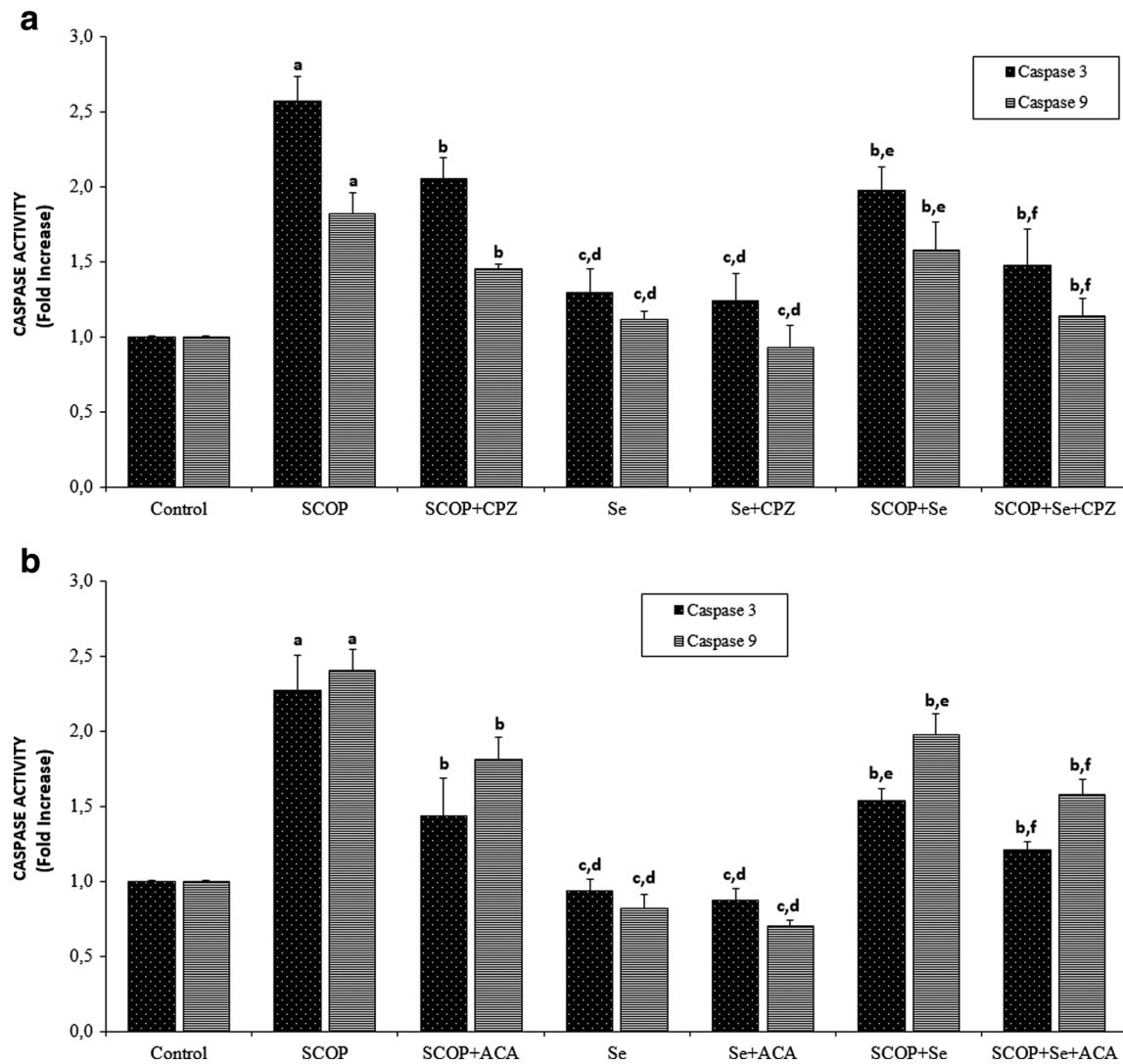


**Fig. 9** Effects of selenium (Se) and SCOP administrations on caspase 3 and 9 activities through TRPV1 (a) and TRPM2 (b) channel activations in hippocampal neurons of rats (mean  $\pm$  SD and  $n=8$ ). The caspase activities were estimated as described under the “Materials and Methods” section. The hippocampal neurons were dissected from in vivo treated animals. Hippocampal neurons of control, SCOP, Se, and SCOP+Se groups were in vitro stimulated in TRPV1 (a) and

TRPM2 (b) experiments by capsaicin (0.01 mM) and CHPx (1 mM), although they were inhibited by CPZ (0.1 mM) and ACA (0.04 mM), respectively. The values are expressed as fold increase over the pretreatment level (experimental/control). (<sup>a</sup> $p < 0.001$  versus control. <sup>b</sup> $p < 0.05$  and <sup>c</sup> $p < 0.001$  versus SCOP group. <sup>d</sup> $p < 0.05$  versus SCOP + CPZ and SCOP + ACA groups. <sup>e</sup> $p < 0.05$  versus Se, Se + CPZ, and Se + ACA groups. <sup>f</sup> $p < 0.05$  versus SCOP + Se groups)

damage in the brain [5, 7]. Our data are consistent with this view: following memory injury induction, lipid peroxidation levels in the hippocampal neurons were significantly ( $p < 0.001$ ) higher in the SCOP group than in the control. However, lipid peroxidation levels in the neurons were significantly ( $p < 0.05$ ) lower in the Se and SCOP+Se groups compared to the SCOP group. GSH-Px activity ( $p < 0.01$ ) and GSH ( $p < 0.001$ ) levels in the hippocampal neurons were significantly lower in the SCOP group than in the control. The GSH and GSH-Px values in the neurons increased in the Se and SCOP+Se groups when compared to the SCOP groups ( $p < 0.001$ ).

### Results of PARP, Procaspase 3, and Procaspase 9 Activities in Hippocampus

Caspase 9 activity is important in the mitochondrial apoptotic cascade, and caspase 3 activity plays an important role in executioner caspase-activated pathways [35, 42]. The procaspases were further processed to caspase 3 and caspase 9 [43, 44]. We assayed procaspase 3 and procaspase 9 as indicators of apoptosis (Fig. 11a). The activities of procaspase 3 and procaspase 9 were significantly ( $p < 0.05$ ) lower in the Se group than in the control and SCOP groups, although they did not differ between the control and SCOP groups.



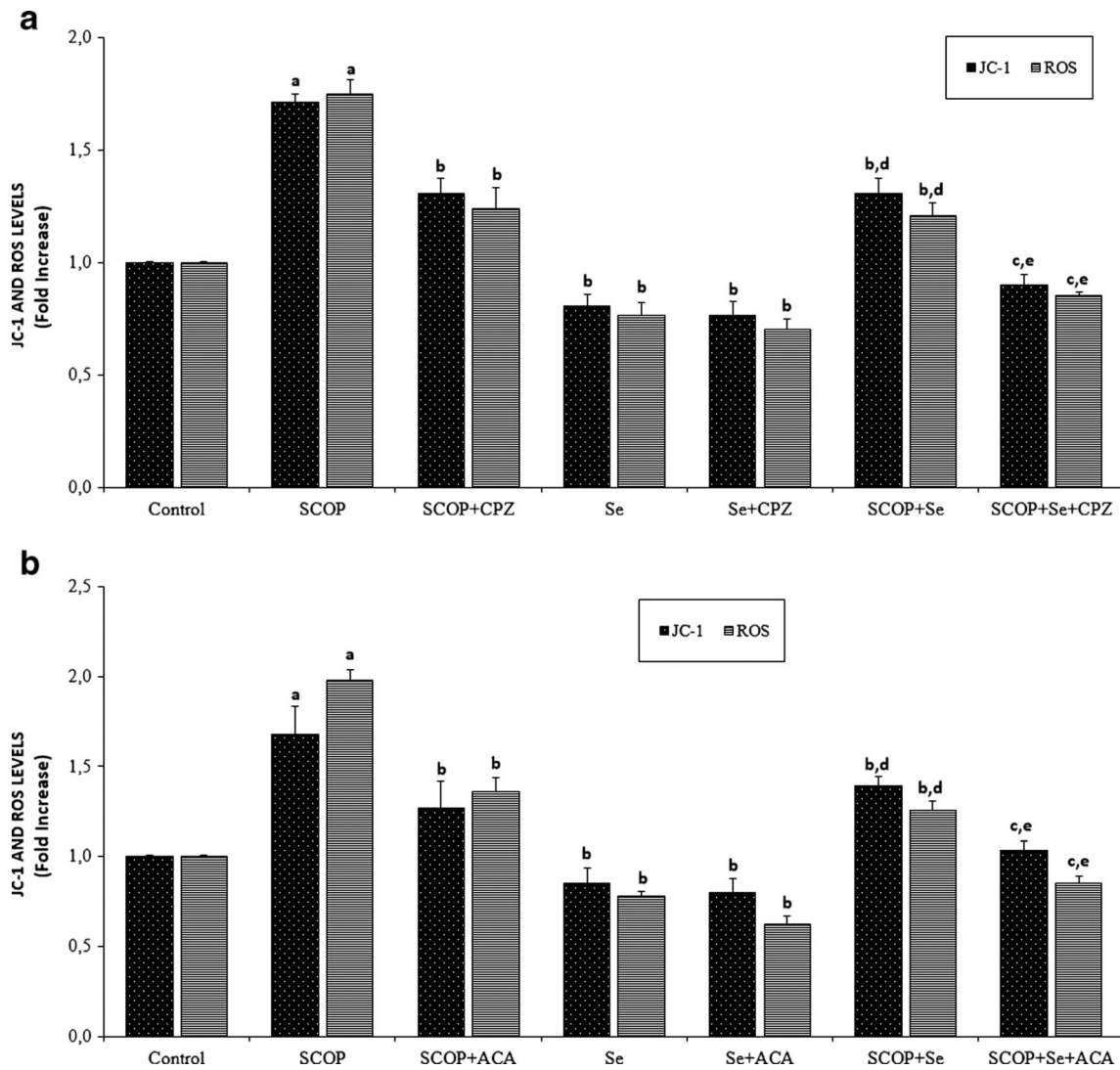


**Fig. 10** Effects of selenium (Se) and SCOP treatments on mitochondrial membrane depolarization (JC-1) and intracellular ROS production through TRPV1 (a) and TRPM2 (b) channel activations in hippocampal neurons of rats (mean  $\pm$  SD and  $n=8$ ). The hippocampal neurons were dissected from *in vivo* treated animals. The hippocampal neurons of control, SCOP, Se, and SCOP + Se groups were *in vitro* stimulated in TRPV1 (a) and TRPM2 (b) experiments by capsaicin (0.01 mM) and CHPx (1 mM), although they were inhibited by CPZ (0.1 mM) and ACA (0.04 mM), respectively. The values are expressed as fold increase over the pretreatment level (experimental/control). (<sup>a</sup> $p < 0.001$  versus control. <sup>b</sup> $p < 0.05$  and <sup>c</sup> $p < 0.001$  versus SCOP group. <sup>d</sup> $p < 0.05$  versus Se, SCOP + CPZ, and SCOP + ACA groups. <sup>e</sup> $p < 0.05$  versus SCOP + Se group.)

**Table 1** The effects of SCOP and selenium treatments on reference memory error (RME) and working memory error (WME) levels in RAM tests of the aged rats (mean  $\pm$  SD and  $n=8$ )

Parameters	Test 1 WME	(Day 0) RME	Test 2 WME	RME	Test 3 WME	RME
Control	0.75 $\pm$ 0.66	2.13 $\pm$ 0.78	0.75 $\pm$ 0.43	2.25 $\pm$ 0.66	–	–
SCOP	0.75 $\pm$ 0.40	1.88 $\pm$ 0.49	1.63 $\pm$ 1.11 <sup>a</sup>	3.38 $\pm$ 0.70 <sup>b</sup>	–	–
Se	0.88 $\pm$ 0.69	3.38 $\pm$ 0.94	0.38 $\pm$ 0.48 <sup>b</sup>	1.75 $\pm$ 1.09 <sup>b</sup>	–	–
SCOP + Se	0.63 $\pm$ 0.45	1.88 $\pm$ 0.83	2.25 $\pm$ 1.07 <sup>b</sup>	4.63 $\pm$ 1.37 <sup>b</sup>	0.63 $\pm$ 0.48 <sup>c</sup>	2.13 $\pm$ 1.36 <sup>c</sup>

RAM test and group details were shown in Fig. 1

<sup>a</sup> $p < 0.05$  versus Test 1

<sup>b</sup> $p < 0.001$  versus Test 1

<sup>c</sup> $p < 0.001$  versus Test 2

**Table 2** The effects of SCOP and selenium treatments on lipid peroxidation, reduced glutathione (GSH) levels, and glutathione peroxidase (GSH-Px) activity in hippocampal neurons of aged rats (mean ± SD)

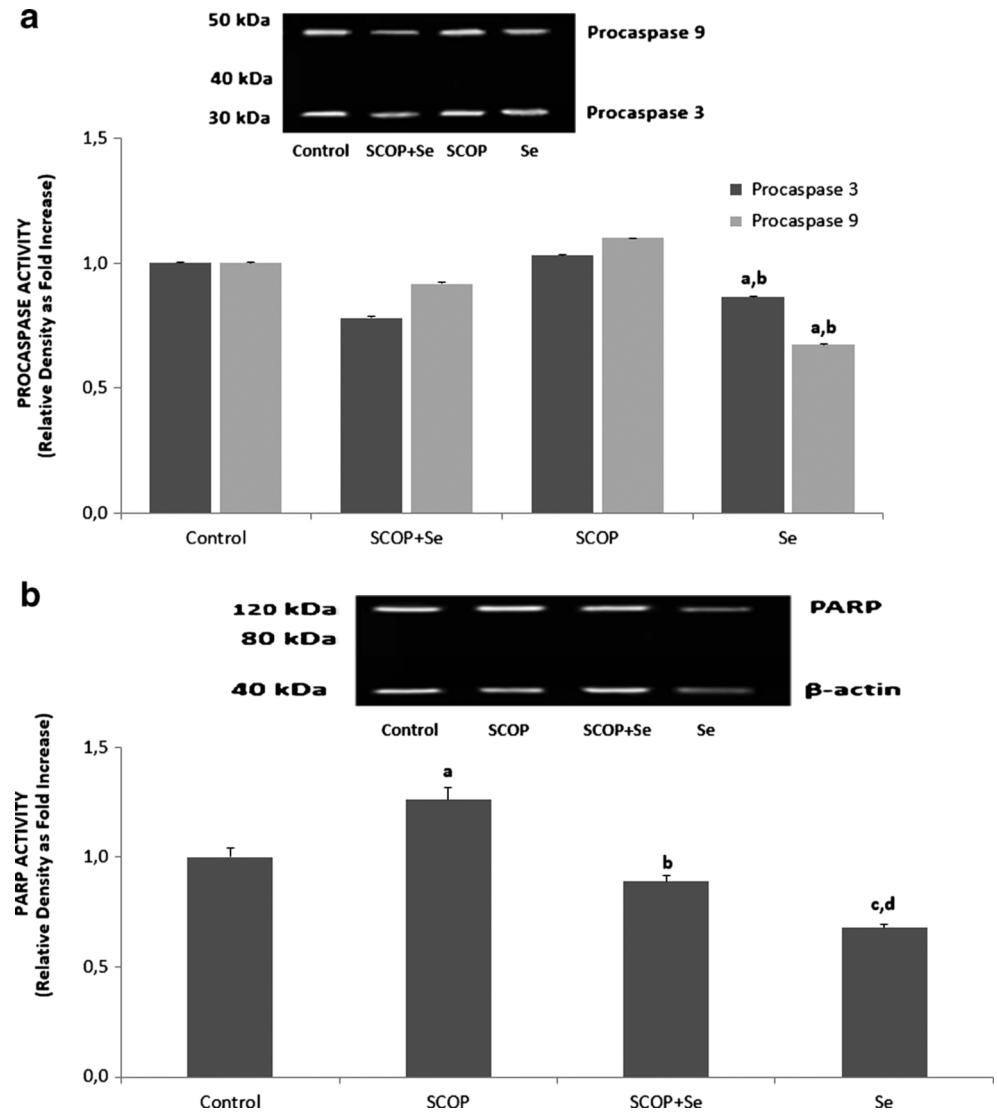
Parameters	Control (n = 8)	SCOP (n = 8)	Se (n = 8)	SCOP + Se (n = 8)
Lipid peroxidation (μmol/g protein)	2.16 ± 0.13	2.77 ± 0.28 <sup>a</sup>	2.39 ± 0.32 <sup>d</sup>	2.44 ± 0.23 <sup>d</sup>
GSH (μmol/g protein)	5.32 ± 0.37	4.54 ± 0.30 <sup>a</sup>	5.57 ± 0.28 <sup>c</sup>	5.49 ± 0.24 <sup>c</sup>
GSH-Px (IU/g protein)	9.80 ± 0.52	8.57 ± 0.76 <sup>b</sup>	10.60 ± 0.57 <sup>c</sup>	10.10 ± 0.91 <sup>c</sup>

<sup>a</sup>*p* < 0.001 versus control  
<sup>b</sup>*p* < 0.01 versus control  
<sup>c</sup>*p* < 0.001 versus SCOP group  
<sup>d</sup>*p* < 0.05 versus SCOP group

PARP is an abundant enzyme in cells indicating and signaling DNA damage to repair mechanisms. Activated in response to single-strand DNA breaks, it subsequently attaches

to regions of injured DNA [10, 11]. TRPM is activated by PARP-induced ADP-ribose production. PARP activities in hippocampal neurons were markedly (*p* < 0.05) higher in the

**Fig. 11** Effects of selenium (Se) administration on procaspase 3, procaspase 9 (Fig. 10b), and PARP activities in the hippocampus of rats. Values are presented as mean ± SD of three separate experiments and expressed relative density (fold increase). (<sup>a</sup>*p* < 0.05 versus control. <sup>b</sup>*p* < 0.05 and <sup>c</sup>*p* < 0.001 versus SCOP group. <sup>d</sup>*p* < 0.05 versus SCOP + Se group)



SCOP group than in the control group (Fig. 11b). However, PARP activities in the neurons were significantly lower in the Se ( $p < 0.001$ ) and SCOP+Se ( $p < 0.05$ ) groups than in the SCOP-only group.

## Discussion

Overactivation of glutamate receptors leads to neuronal death in many neurodegenerative diseases, including AD with dementia [2, 3]. The results of our limited study provide clues about the TRPM2 [8–10] and TRPV1 [23, 25, 26] channels in neurons' memory impairment in AD and dementia models. In addition, one of the main causes of neurodegenerative diseases is excessive production of oxidative stress with an overload of  $\text{Ca}^{2+}$  entry through increased mitochondrial membrane depolarization, along with TRPM2 and TRPV1 channel activity [5–7, 18]. Our results confirm previous data indicating that selenium prevents capsaicin and oxidative stress-induced excitotoxicity in rat neuronal cultures [18, 29]. Recent studies have suggested that selenium in neurons and cell cultures could preferentially block the TRPM2 and TRPV1 channels, scavenging ROS [29, 30]. Looking at the results discussed above, we suggest that SCOP-dependent alterations of  $\text{Ca}^{2+}$  influx through cation channels, mitochondrial function, and oxidative stress induced parallel pathophysiological mechanisms in memory impairment. Impaired memory signaling and  $\text{Ca}^{2+}$  influx through TRP channel activations trigger sensory neuron mitochondrial depolarization in this process [18, 29]. The successive increase in mitochondrial depolarization induces further ROS production and disrupts  $\text{Ca}^{2+}$  homeostatic mechanisms, particularly TRPM2 and TRPV1 channels [2].

Amyloid-beta peptide and tau proteins are the main constituents of senile plaques in AD and dementia [1, 2]. SCOP induces overproduction of amyloid-beta peptide and tau proteins in neurons [42]. Meanwhile, the proteins are also the main source of mitochondrial oxidative stress and glutathione depletion in the diseases [9, 43]. Some researchers have reported evidence of amyloid-beta fibrils in neurons, leading to calcium influx through activation of TRPM2 and TRPV1 channels and neuronal death associated with overloaded  $\text{Ca}^{2+}$  entry and oxidative stress [8–10]. Apart from the direct role in cell death, amyloid-beta-mediated antioxidant GSH and GSH-Px depletion can lead to synaptic dysfunction, resulting in excitotoxic neurodegeneration during memory impairment [7]. GSH and GSH-Px contain cysteine groups in their structure. Results reported in recent papers indicate that oxidation of cysteine groups and depletion of GSH play an important role in the activation of TRPM2 and TRPV1 channels in neurons [11, 12, 22]. To our knowledge, no studies have reported on the role of selenium in the hippocampus and DRG of aged rats with memory impairment. However,

studies have shown that selenium treatment decreases TRPM2 and TRPV1 channel activities in Chinese hamster ovary cells [29], human neutrophils [30], DRG, and hippocampal neurons [18]. Recently, we have observed the modulator role of selenium on GSH, GSH-Px, TRPM2, and TRPV1 channels in the DRG and hippocampus of diabetic rats [18]. We observed that SCOP-induced memory impairment is characterized by increased oxidative stress,  $\text{Ca}^{2+}$  influx, and apoptosis. However, treatment with selenium exerts beneficial effects on hippocampal and DRG neuron values in rats with SCOP-induced memory impairment. Data from the SCOP groups support the idea that capsaicin acts by initiating metabolic pathways, resulting in the production of a cytosolic factor, such as the products of oxidative stress and decreased GSH and GSH-Px which is responsible for the activation of TRPM2 and TRPV1 [22].

$[\text{Ca}^{2+}]_i$  accumulation has been presented as a key regulator of cell survival, but this ion can also induce apoptosis in neuronal death [44]. In addition, mitochondria have a  $\text{Ca}^{2+}$  buffering capacity by sequestering excess  $\text{Ca}^{2+}$  from the cytosol [37, 38]. Overloaded  $[\text{Ca}^{2+}]_i$  concentration of mitochondria can induce an apoptotic program by stimulating the release of apoptosis-promoting factors, such as cytochrome c, and by generating ROS due to respiratory chain damage [45]. If mitochondrial membrane depolarization occurs in the hippocampus, it activates excessive ROS production and apoptotic pathways, such as caspase 3 and caspase 9. We have provided compelling evidence to support the belief that SCOP-induced mitochondrial  $\text{Ca}^{2+}$  uptake evoked by rises in  $[\text{Ca}^{2+}]_i$  induces mitochondrial membrane depolarization, excessive ROS production, and apoptosis. Our results indicate that the blockade of both  $\text{Ca}^{2+}$  uptake into mitochondria with selenium, TRPM2 (ACA), and TRPV1 (CPZ) antagonists as well as increases in  $[\text{Ca}^{2+}]_i$  were able to decrease mitochondrial membrane depolarization, excessive ROS production, and apoptosis mediated by CHPx and capsaicin, which was able to block  $\text{Ca}^{2+}$  entry from outside the neurons into the cytosol.

In conclusion, in our memory impairment experimental model, TRPM2 and TRPV1 channels are involved in  $\text{Ca}^{2+}$  entry-induced neuronal death in the hippocampal and DRG neurons; meanwhile, reduced channel activity by selenium treatment may account for their neuroprotective activity against apoptosis and  $\text{Ca}^{2+}$  entry. Selenium treatment also increased memory impairment indicators (WME and RME), GSH level, and GSH-Px activity in the neurons. These findings hold particular significance and may provide an explanation for SCOP-induced neuronal death and selenium's memory impairment-reducing properties through endogenous oxidative stress pathways. It seems that TRPM2 and TRPV1 channels may become important pharmacological targets in the

treatment of memory impairment-induced oxidative hippocampal injury.

**Acknowledgments** The authors wish to thank researcher Bilal Çiğ and technicians Fatih Şahin and Muhammet Şahin (Neuroscience Research Center, SDU, Isparta, Turkey) for helping with the  $[Ca^{2+}]_i$  (Fura-2AM), patch-clamp, lipid peroxidation, and antioxidant analyses. The abstract of the study will be partially published in the “8th International Congress on Psychopharmacology & 4th International Symposium on Child and Adolescent Psychopharmacology, April 20–24, 2016, in Antalya, Turkey.”

**Financial Disclosure** The study was supported by the Unit of Scientific Research Project (BAP), Süleyman Demirel University, Isparta, Turkey (Project Number BAP: 4257-TU-15). There is no financial disclosure for the current study.

**Authorship Contributions** MN and KD formulated the hypothesis and were responsible for writing the report. İSO and HB were also responsible for the animal experiments such as the induction of memory injury through SCOP administration and injection of selenium. İSÖ performed the  $Ca^{2+}$  analyses Western blot, apoptosis, and mitochondrial depolarization analyses.

**Compliance with Ethical Standards** The study was approved by the Local Experimental Animal Ethical Committee of Suleyman Demirel University (SDU) (protocol number 10.02.2015-03).

**Conflict of Interest** The authors declare that they have no conflicts of interest.

**Human and Animal Rights and Informed Consent** All research procedures and animal care complied with the guidelines of the International Association Study Plan for induction of memory injury. The animals were maintained and used according to the Animal Welfare Act and the Guide for the Care and Use of Laboratory.

## References

- LaFerla FM (2002) Calcium dyshomeostasis and intracellular signalling in Alzheimer's disease. *Nat Rev Neurosci* 3:862–872
- Pascale A, Etcheberrigaray R (1999) Calcium alterations in Alzheimer's disease: pathophysiology, models and therapeutic opportunities. *Pharmacol Res* 39:81–88
- Nishimura I, Takazaki R, Kuwako K, Enokido Y, Yoshikawa K (2003) Upregulation and antiapoptotic role of endogenous Alzheimer amyloid precursor protein in dorsal root ganglion neurons. *Exp Cell Res* 286:241–251
- Kurz AF (2005) Uncommon neurodegenerative causes of dementia. *Int Psychogeriatr* 17(Suppl 1):S35–49
- Paula-Lima AC, Adasme T, Hidalgo C (2014) Contribution of  $Ca^{2+}$  release channels to hippocampal synaptic plasticity and spatial memory: potential redox modulation. *Antioxid Redox Signal* 21:892–914
- Alberdi E, Sánchez-Gómez MV, Cavaliere F, Pérez-Samartín A, Zugaza JL, Trullas R, Domercq M, Matute C (2010) Amyloid beta oligomers induce  $Ca^{2+}$  dysregulation and neuronal death through activation of ionotropic glutamate receptors. *Cell Calcium* 47:264–272
- Zhou WW, Lu S, Su YJ, Xue D, Yu XL, Wang SW, Zhang H, Xu PX, Xie XX, Liu RT (2014) Decreasing oxidative stress and neuroinflammation with a multifunctional peptide rescues memory deficits in mice with Alzheimer disease. *Free Radic Biol Med* 74:50–63
- Fonfria E, Marshall IC, Boyfield I, Skaper SD, Hughes JP, Owen DE, Zhang W, Miller BA, Benham CD, McNulty S (2005) Amyloid beta-peptide(1–42) and hydrogen peroxide-induced toxicity are mediated by TRPM2 in rat primary striatal cultures. *J Neurochem* 95:715–723
- Ostapchenko VG, Chen M, Guzman MS, Xie YF, Lavine N, Fan J, Beraldo FH, Martyn AC, Belrose JC, Mori Y, MacDonald JF, Prado VF, Prado MA, Jackson MF (2015) The Transient receptor potential melastatin 2 (TRPM2) channel contributes to  $\beta$ -amyloid oligomer-related neurotoxicity and memory impairment. *J Neurosci* 35:15157–15169
- Naziroğlu M, Dikici DM, Dursun S (2012) Role of oxidative stress and  $Ca^{2+}$  signaling on molecular pathways of neuropathic pain in diabetes: focus on TRP channels. *Neurochem Res* 37:2065–2075
- Naziroğlu M (2011) TRPM2 cation channels, oxidative stress and neurological diseases: where are we now? *Neurochem Res* 36:355–366
- Naziroğlu M (2009) Role of selenium on calcium signaling and oxidative stress-induced molecular pathways in epilepsy. *Neurochem Res* 34:2181–2191
- Schweizer U, Bräuer AU, Köhrle J, Nitsch R, Savaskan NE (2004) Selenium and brain function: a poorly recognized liaison. *Brain Res Brain Res Rev* 45:164–178
- Rita Cardoso B, Silva Bandeira V, Jacob-Filho W, Franciscato Cozzolino SM (2014) Selenium status in elderly: relation to cognitive decline. *J Trace Elem Med Biol* 28:422–6
- Vural H, Demirin H, Kara Y, Eren I, Delibas N (2010) Alterations of plasma magnesium, copper, zinc, iron and selenium concentrations and some related erythrocyte antioxidant enzyme activities in patients with Alzheimer's disease. *J Trace Elem Med Biol* 24:169–173
- Lakshmi BV, Sudhakar M, Prakash KS (2015) Protective effect of selenium against aluminum chloride-induced Alzheimer's disease: behavioral and biochemical alterations in rats. *Biol Trace Elem Res* 165:67–74
- Uğuz AC, Naziroğlu M (2012) Effects of selenium on calcium signaling and apoptosis in rat dorsal root ganglion neurons induced by oxidative stress. *Neurochem Res* 37:1631–1638
- Kahya MC, Naziroğlu M, Çiğ B. Modulation of diabetes-induced oxidative stress, apoptosis, and  $Ca^{2+}$  entry through TRPM2 and TRPV1 channels in dorsal root ganglion and hippocampus of diabetic rats by melatonin and selenium. *Mol Neurobiol*. 2016 [Epub ahead of print]. DOI 10.1007/s12035-016-9727-3.
- Caterina MJ, Schumacher MA, Tominaga M, Rosen TA, Levine JD, Julius D (1997) The capsaicin receptor: a heat-activated ion channel in the pain pathway. *Nature* 389:816–824
- Perraud AL, Fleig A, Dunn CA, Bagley LA, Launay P, Schmitz C, Stokes AJ, Zhu Q, Bessman MJ, Penner R, Kinet JP, Scharenberg AM (2001) ADP-ribose gating of the calcium-permeable LTRPC2 channel revealed by Nudix motif homology. *Nature* 411:595–599
- Naziroğlu M, Lückhoff A (2008) A calcium influx pathway regulated separately by oxidative stress and ADP-Ribose in TRPM2 channels: single channel events. *Neurochem Res* 33:1256–1262
- Shimizu S, Takahashi N, Mori Y (2014) TRPs as chemosensors (ROS, RNS, RCS, gasotransmitters). *Handb Exp Pharmacol* 223:767–794
- Cristino L, de Petrocellis L, Pryce G, Baker D, Guglielmotti V, Di Marzo V (2006) Immunohistochemical localization of cannabinoid type 1 and vanilloid transient receptor potential vanilloid type 1 receptors in the mouse brain. *Neuroscience* 139:1405–1415
- Bai JZ, Lipski J (2010) Differential expression of TRPM2 and TRPV4 channels and their potential role in oxidative stress-induced cell death in organotypic hippocampal culture. *Neurotoxicology* 31:204–214



25. Gupta S, Sharma B (2014) Pharmacological benefits of agomelatine and vanillin in experimental model of Huntington's disease. *Pharmacol Biochem Behav* 122:122–35
26. Gupta S, Sharma B, Singh P, Sharma BM (2014) Modulation of transient receptor potential vanilloid subtype 1 (TRPV1) and nor-epinephrine transporters (NET) protect against oxidative stress, cellular injury, and vascular dementia. *Curr Neurovasc Res* 11:94–106
27. Park L, Wang G, Moore J, Girouard H, Zhou P, Anrather J, Iadecola C (2014) The key role of transient receptor potential melastatin-2 channels in amyloid- $\beta$ -induced neurovascular dysfunction. *Nat Commun* 5:5318
28. Jiang X, Jia LW, Li XH, Cheng XS, Xie JZ, Ma ZW, Xu WJ, Liu Y, Yao Y, Du LL, Zhou XW (2013) Capsaicin ameliorates stress-induced Alzheimer's disease-like pathological and cognitive impairments in rats. *J Alzheimers Dis* 35:91–105
29. Nazırođlu M, Özgöl K, Küçükayaz M, Çiđ B, Hebeisen S, Bal R (2013) Selenium modulates oxidative stress-induced TRPM2 cation channel currents in transfected Chinese hamster ovary cells. *Basic Clin Pharmacol Toxicol* 112:96–102
30. Köse SA, Nazırođlu M (2014) Selenium reduces oxidative stress and calcium entry through TRPV1 channels in the neutrophils of patients with polycystic ovary syndrome. *Biol Trace Elem Res* 158:136–142
31. Chen C, Li XH, Zhang S, Tu Y, Wang YM, Sun HT (2014) 7,8-dihydroxyflavone ameliorates scopolamine-induced Alzheimer-like pathologic dysfunction. *Rejuvenation Res* 17:249–254
32. Neha X, Sodhi RK, Jaggi AS, Singh N (2014) Animal models of dementia and cognitive dysfunction. *Life Sci* 109:73–86
33. Hritcu L, Stefan M, Brandsch R, Mihasan M (2015) Enhanced behavioral response by decreasing brain oxidative stress to 6-hydroxyl-nicotine in Alzheimer's disease rat model. *Neurosci Lett* 591:41–7
34. Uđuz AC, Nazırođlu M, Espino J, Bejarano I, González D, Rodríguez AB, Pariente JA (2009) Selenium modulates oxidative stress-induced cell apoptosis in human myeloid HL-60 cells through regulation of calcium release and caspase-3 and -9 activities. *J Membr Biol* 232:15–23
35. Gryniewicz C, Poenie M, Tsien RY (1985) A new generation of  $Ca^{2+}$  indicators with greatly improved fluorescence properties. *J Biol Chem* 260:3440–3450
36. Espino J, Bejarano I, Redondo PC, Rosado JA, Barriga C, Reiter RJ, Pariente JA, Rodríguez AB (2010) Melatonin reduces apoptosis induced by calcium signaling in human leukocytes: evidence for the involvement of mitochondria and Bax activation. *J Membr Biol* 233:105–118
37. Espino J, Bejarano I, Paredes SD, Barriga C, Rodríguez AB, Pariente JA (2011) Protective effect of melatonin against human leukocyte apoptosis induced by intracellular calcium overload: relation with its antioxidant actions. *J Pineal Res* 51:195–206
38. Bejarano I, Redondo PC, Espino J, Rosado JA, Paredes SD, Barriga C, Reiter RJ, Pariente JA, Rodríguez AB (2009) Melatonin induces mitochondrial-mediated apoptosis in human myeloid HL-60 cells. *J Pineal Res* 46:392–400
39. Placer ZA, Cushman L, Johnson BC (1966) Estimation of products of lipid peroxidation (malonyl dialdehyde) in biological fluids. *Analytical Biochem* 16:359–364
40. Sedlak J, Lindsay RHC (1968) Estimation of total, protein bound and non-protein sulfhydryl groups in tissue with Ellmann's reagent. *Analytical Biochem* 25:192–205
41. Lawrence RA, Burk RF (1976) Glutathione peroxidase activity in selenium-deficient rat liver. *Biochem Biophys Res Com* 71:952–958
42. Bihagi SW, Singh AP, Tiwari M (2012) Supplementation of *Convolvulus pluricaulis* attenuates scopolamine-induced increased tau and amyloid precursor protein ( $A\beta$ PP) expression in rat brain. *Indian J Pharmacol* 44:593–598
43. Barbero-Camps E, Fernández A, Martínez L, Fernández-Checa JC, Colell A (2013) APP/PS1 mice overexpressing SREBP-2 exhibit combined  $A\beta$  accumulation and tau pathology underlying Alzheimer's disease. *Hum Mol Genet* 22:3460–3476
44. Kumar VS, Gopalakrishnan A, Nazırođlu M, Rajanikant GK (2014) Calcium ion—the key player in cerebral ischemia. *Curr Med Chem* 21:2065–2075
45. Hajnóczky G, Csordás G, Das S, Garcia-Perez C, Saotome M, Sinha Roy S, Yi M (2006) Mitochondrial calcium signalling and cell death: approaches for assessing the role of mitochondrial  $Ca^{2+}$  uptake in apoptosis. *Cell Calcium* 40:553–560